PROBABILISTIC NEURAL NETWORKS FOR SEGMENTATION OF FEATURES IN CORN KERNEL IMAGES

L. W. Steenhoek, M. K. Misra, W. D. Batchelor, J. L. Davidson

ABSTRACT. *A method is presented for clustering of pixel color information to segment features within corn kernel images. Features for blue–eye mold, germ damage, sound germ, shadow in sound germ, hard starch, and soft starch were identified by red, green, and blue (RGB) pixel value inputs to a probabilistic neural network. A data grouping method to obtain an exemplar set for adjustment of the Probabilistic Neural Network (PNN) weights and optimization of a universal smoothing factor is described. Of the 14,427 available exemplars (RGB pixel values sampled from previously collected images), 778 were used for adjustment of the network weights, 737 were used for optimization of the PNN smoothing parameter, and 12,912 were reserved for network validation. Based on a universal PNN smoothing factor of 0.05, the network was able to provide an overall pixel classification accuracy of 86% on calibration data and 75% on unseen data. Much of the misclassification was due to overlap of pixel values among classes. When an additional network layer was added to combine similar classes (blue–eye mold and germ damage, sound germ and shadow in sound germ, and hard and soft starch), network results were significantly enhanced so that accuracy on validation data was 94.7%. Image quality was shown to be important to the success of this algorithm as lighting and camera depth of field effects caused artifacts in the segmented images.*

Keywords. *Grain damage, Evaluation, Machine vision, Probabilistic, Neural network, Corn, Color, Pattern recognition.*

Most corn kernel damage in Midwestern U.S. growing regions is due to either germ or blue–eye mold damage (Steenhoek et al., 2001). In this article, a method for segmentation of damaged areas in corn kernel images using neural network pattern recognition techniques is developed. This segmentation method is used in Steenhoek et al. (2001) to classify kernels into blue–eye mold, germ damage, or sound categories.

For a computer vision system to classify corn kernel images, it is necessary to first preprocess or segment those images into separate areas representing categories such as mold, germ damage, sound germ, hard and soft starch, etc.

Several researchers have investigated the use of image processing for identification of features of interest in biological products. Panigrahi et al. (1998) used linear discriminate analysis to classify edible soybean images into light, medium, and dark color groups using normalized red, green, blue (RGB) and hue, saturation, intensity (HSI) color coordinates. Ng et al. (1998) developed a color calibration method and a back–propagation neural network applied to RGB pixel values to identify mold and nonmold pixels in corn kernel images. Gao et al. (1995) applied two color segmentation techniques for meat images: a threshold window based on standard deviations from the mean, and a Mahalanobis distance criterion on each of the RGB color histograms. The Mahalanobis distance method provided the best results. A pixel clustering technique was used by Klinker et al. (1988) to separate image pixels based on color. The procedure was to project all pixels from an image containing objects of different color into three–dimensional RGB space and then use the cluster analysis methods to identify and distinguish between areas of different colors in the image.

Article was submitted for review in May 1999; approved for publication by the Information & Electrical Technologies Division of ASAE in September 2000. Presented at the 1999 ASAE Annual Meeting as Paper No. 99–3198.

This article was edited as Journal Paper No. J–18288 of the Iowa Agriculture and Home Economics Experiment Station, Ames, Iowa. Project No. 2901, and supported by Hatch Act and State of Iowa Funds.

The authors are **Loren W. Steenhoek,** ***ASAE Member Engineer,*** Technology Integration Project Leader, Pioneer Hi–Bred, **Manjit K. Misra**, ***ASAE Member Engineer***, Director, Seed Science Center, **William D. Batchelor**, ***ASAE Member Engineer***, Associate Professor, Ag and Biosystems Engineering Department, **Jennifer L. Davidson**, Associate Professor, Electrical and Computer Engineering Department, Iowa State University, Ames, Iowa. **Corresponding author:** L. Steenhoek, Pioneer Hi–Bred; 6900 N.W. 62nd; Johnston, IA 50131; phone: 515–270–3983; fax: 515–270–3411; e–mail: loren.steenhoek@pioneer.com.

PROBABILISTIC NEURAL NETWORK (PNN) MODEL

There are many neural network architecture models. Lippmann (1987), Hush and Horne (1993), Rumelhart et al. (1994), Widrow and Lehr (1990), and others have described theories of these varied architectures. Perhaps the most popular network model is the classical multilayer perceptron method (Rumelhart and McClelland, 1986), which has been applied to many agricultural problems (McClendon and Batchelor, 1995; Panigrahi et al., 1994; Dowell, 1994; Jia, 1993). Among the weaknesses of the back propagation network are sensitivity to variations in training data, difficulties in choosing the number of hidden nodes and learning rate (Batchelor et al., 1997), susceptibility to false minima, and length of learning time required. Other approaches have included Learning Vector Quantization

(LVQ) or Kohonen Networks (Ahmad et al., 1993; Yie et al., 1993; Panigrahi and Marsh, 1996), Radial Basis Function networks, and Discriminate Function approaches (Precetti and Krutz, 1993a,b). One additional network architecture that has not been published widely in the agricultural literature is the Probabilistic Neural Network (PNN) popularized by D.F. Specht (1988, 1990, 1996).

For the generalized problem with distinctly separable data, the PNN essentially works as a look–up table, providing a response to new input patterns that is similar to the response of training patterns closest to the new input feature space. It is referred to as a memory–based model, because it represents generalizations of the inputs, which "memorize" responses to the training data. A probability density estimate is established via a Gaussian window placed at every training sample so that a non–zero response is output over a localized region of the input space. Training patterns determine the window positions and responses so that new inputs will generate a response that is similar to the response generated by the training data that they resemble (Hush and Horne, 1993). As with other pattern recognition techniques, PNNs require that training data be available from the entire solution space domain. A PNN can be trained with sparse data but cannot interpolate between missing classification patterns.

PNNs are feed forward neural networks and respond to an input pattern by processing the input data from one layer to the next with no feedback paths. An inherent advantage of the PNN architecture is that it can be made to respond only to inputs that are in the same region of the training data input space. Inputs outside the learning area can be flagged, thus avoiding extrapolation errors. Furthermore, training the network to have a proper response in a part of measurement space does not disturb the trained response in other distant parts of the measurement space. Other advantages include:

- PNNs train quickly as only one pass through the data is required.
- PNNs have only one free parameter, the smoothing factor, to be adjusted by the user and this factor can be adjusted at run time without the requirement of network retraining.
- Shape of the decision surface can be made as complex as necessary. It can also be made very simple by choosing appropriate values for the smoothing factor.
- Sparse samples are adequate for network performance.
- Results are not dependent on randomization order of training data.
- Training can be incremental as data becomes available and old patterns can be "forgotten" and replaced by new patterns if so desired.

A major disadvantage of the PNN architecture is that it requires one node or neuron for each training exemplar. For large training data sets, this disadvantage presents a computational problem as a large computer memory is required and the amount of computation necessary to classify an unknown point at run time is proportional to the size of the training set. Both of these issues, however, are becoming less important as computer technology advances.

A detailed derivation of the probabilistic neural network is developed in Specht (1988, 1990, 1996) and Masters (1993, 1995). The discussion that follows is intended to summarize Specht's derivation and provide the readers of this article with a very generalized outline of the probabilistic neural network principles.

Statistically paralleled by kernel discriminant analysis, probabilistic neural networks are based on the Bayesian strategy for pattern recognition, which postulates that a decision rule to classify patterns should minimize "expected risk" of misclassification. If the probability density functions for categories Θ_A, Θ_B, … , Θ_N can be defined by $f_A[X]$, $f_B[X]$, …, $f_N[X]$, then the a priori probability (h_A, h_B, …, h_N) of occurrence of patterns from each category and the loss associated with misclassification (l_A, l_B, …, l_N) can be used to develop the decision rule relationship shown in equation 1 where d(X) is a classification function for the input vector X.

$$d(X) = \Theta_k \text{ if } h_k l_k f_k [X] < h_q l_q f_q [X] \text{ for all } k \neq q \quad (1)$$

The accuracy of decision boundaries depends on the accuracy with which the underlying probability density functions ($f_A[X]$, $f_B[X]$, … , $f_N[X]$) are estimated. Cacoullos (1966) suggested a Gaussian kernel that expresses a multivariate estimate of the probability density function:

$$f_k[X] = \frac{1}{2\pi^{p/2}\sigma^p}\frac{1}{m} \sum_{i=1}^{m} \exp\left[-\frac{(X - X_{ki})^t (X - X_{ki})}{2\sigma^2}\right] \quad (2)$$

where

k = category
i = pattern number
m = total number of training patterns
X_{ki} = i^{th} training pattern from category k
σ = smoothing parameter
p = dimensionality of measurement space

In equation 2, $f_K[X]$ is simply the sum of small multivariate Gaussian distributions centered at each of the training samples. The variable σ is a smoothing factor that, in effect, determines the Gaussian window width and the degree of interpolation between points. For the two–dimensional input case shown in figure 1, a small value of σ gives distinct modes corresponding to the locations of training samples. As the value of σ increases, the degree of interpolation also increases. Some experimentation is required to determine the smoothing factor that is best for each data set; however, no retraining is required as it is applied at run–time. Ward Systems Group (1993) suggests a

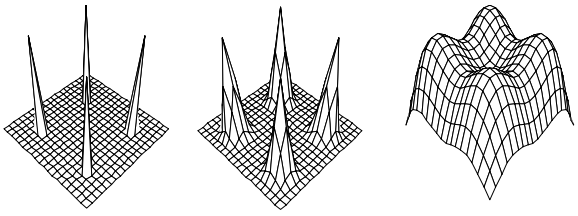

Figure 1. The smoothing effect of different values of σ (Specht, 1996).

smoothing factor range of 0.01 to 1 for good results. In this article, an optimal value of σ was determined by computational iteration.

As with other types of feed–forward networks, the PNN is built upon several layers of neuron units. Figure 2 shows the PNN architecture for a two–category classification. For the generalized case, the input vector X is normalized to unit length and fed into the input unit neurons. Pattern units in the second layer are joined to the input layer by weights that form a natural dot product with the input vector. Thus $Z_i = X \cdot W_i$. If the nonlinear operation $\exp[(Z_i - 1)/\sigma^2]$ is then applied, the result is equivalent to that derived using equation 2, and is in the same form as equation 3.

$$\exp\left[-\frac{(W_i - x)^t (W_i - x)}{2\sigma^2}\right] \quad (3)$$

In the third layer, summation unit neurons add the inputs from pattern units that correspond to the categories from which training patterns were selected. The network is trained by setting the W_i weight vector in one of the pattern units equal to each of the X patterns in the training set and then connecting the pattern unit's output to the appropriate summation unit. The output rule is a winner–take–all function of the summation units. A separate neuron (pattern unit) is required for every training pattern. Training is a one–pass operation. Sensitivity of the network is then adjusted by selecting an optimal smoothing factor.

This article describes implementation of the most generalized form of PNN. More advanced versions, which optimize the smoothing factor via statistical and genetic techniques, have been developed (Masters 1993, 1995; Ward Systems Group, 1997) and are implemented in Chtioui et al. (1996, 1998) and Steenhoek et al. (2001).

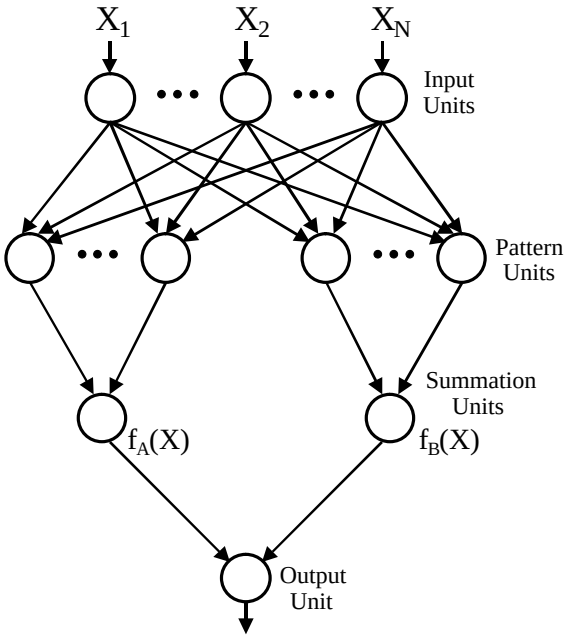

Figure 2. PNN architecture (Specht, 1996).

Objective

The objective of this study was to develop and test an image–processing algorithm for segmentation of damaged and sound areas within corn kernel images using a probabilistic neural network and color pattern recognition techniques.

Materials and Methods

The hypothesis of this experiment was that corn kernel damage categories can be recognized by repeatable color patterns and the color patterns can be used to segment areas in corn kernel images. Thus, a procedure was developed to collect RGB pixel values from areas representing several attribute categories and to use the values for training of a neural network for image segmentation.

Corn Kernal Images

Selection of corn kernel samples, development of a machine vision system, and acquisition of the corn kernel images are described in Steenhoek et al. (2001). Briefly, 720 kernels classified in roughly equal proportions of undamaged, germ–damaged, and blue–eye mold–damaged categories were collected from 24 handpicked sample lots. Each of the 720 kernels was assigned a randomly generated kernel identification code and placed in an individual plastic bag. All kernels were inspected by four members of the Federal Grain Inspection Service (FGIS) Board of Appeals and Review and assigned to categories of blue–eye mold–damaged, germ–damaged, and sound. Three replicate images of each of the 720 kernels (2,160 total images) were obtained using an RGB color camera, a diffuse lighting chamber, and a Sharp GPB–2 image processing system.

Feature Attribute Categories

In this study, the ultimate goal was to categorize kernel images as blue–eye mold–damaged, germ–damaged, and sound. Therefore, attributes that were related to these kernel classifications needed to be identified. These attributes were pixel regions representing germ damage, blue–eye mold damage, sound germ, and starch. Because typical corn kernels contain both hard and soft starch endosperm, with each type of starch having different color intensity, categories for both hard starch and soft starch were chosen. In addition, the three–dimensional nature of corn kernels often caused areas of shadow to appear in the germ. To alleviate the concern that the dark appearance of shadows in the sound germ areas could be misidentified as a damaged area, an additional category for shadow in sound germ was chosen. Thus, six categories (blue–eye mold, germ damage, shadow in sound germ, sound germ, hard starch, and soft starch) were used in classification.

Use of Kernel Edge Pixel Samples for Background Segmentation

Due to the three–dimensional nature of corn kernels, even with the best lighting conditions, shadows and a gradient descent of pixel values occurred in the pixels immediately surrounding the kernel edge. Four pixels from this area were sampled from each of the sound kernels to determine the distribution of pixel level values at the kernel edge. This

information was obtained for selection of a suitable threshold used to separate the kernel from black background. The kernel edge pixel region in the images was approximately 3 pixels wide.

Acquisition of Color Pattern Samples

The goal of sample collection was to obtain representative exemplars for distinct color patterns. Pixel samples were collected only from images of kernels having consensus opinions from each of the four FGIS inspectors. The six color pattern categories used in attribute segmentation and kernel edge used for background segmentation are illustrated in figure 3 and described in table 1. These categories, not to be confused with overall kernel classification (i.e., blue–eye mold–damaged, germ–damaged, and sound), were for individual pixels inside the kernels that represented color patterns related to overall kernel classification. Four pixel samples were collected for each attribute and associated image whenever possible as detailed in table 2. Some images did not have distinctly identifiable attributes related to a particular class, and, therefore, no data was collected. Pixel samples for which red, green, or blue pixel values were equal to 255 (sensor saturation) were also ignored.

Software was developed to extract red, green, and blue pixel values from regions representing color pattern features from each of the collected images. Recorded information for each selected pixel included the following: x and y pixel position, image file name, image kernel code, color pattern category, and RGB pixel values. A total of 14,427 pixel samples were collected from the database of 2,160 images. A breakdown of the number of valid pixel samples collected from each attribute category is given in table 3.

Data for Network Training

Of the 14,427 valid pixel samples, 778 were flagged for network training and 737 were marked for adjustment of the smoothing factor, leaving 12,912 for validation. The pixel samples collected from each attribute category were grouped into low, medium, and high levels over each of the RGB color bands Steenhoek (1999). Inasmuch as the original data were essentially normally distributed, a measure of 0.5 standard deviation (σ_x) above or below the mean (X) was used to divide the data into three approximately equal levels for each color plane and attribute category according to equation 4.

$$f(X)=\begin{Bmatrix}\text{Low if } X < (\overline{X} - 0.5\sigma_x)\\ \text{Med if } (\overline{X} - 0.5\sigma_x) < X < (\overline{X} + 0.5\sigma_x)\\ \text{High if } X > (\overline{X} + 0.5\sigma_x)\end{Bmatrix} \quad (4)$$

Selecting all pixel samples within each color group and sorting the resulting record set by kernel identification code created a training set. For the first 10 records, a flag was set to reserve those records for training. The next 10 records were flagged for optimization of the smoothing parameter, and the remaining records were marked for validation.

PNN Application for Image Segmentation

The probabilistic neural network architecture is illustrated in figure 4. Red, green, and blue pixel values were used as inputs with output categories corresponding to the probability that a pixel sample would fall into one of the six categories For each network output, a value between 0 and 1 represented the network's predicted probability for that category.

The probabilistic neural network algorithm implemented in the NeuroWindows dynamic link library (Ward Systems Group, 1993) was used for training and validation of the network described previously. First, the network was trained using the 778 pixel samples that had been flagged for training. Then, a universal smoothing factor for all network inputs was selected by applying smoothing factor values ranging from 0.001 to 10 to the 737 pixel samples that had been flagged for smoothing factor adjustment. As implemented in the NeuroWindows library, this smoothing factor had equal effect on each of the red, green, and blue network inputs. The criterion was to minimize the error in percent classification for the smoothing dataset.

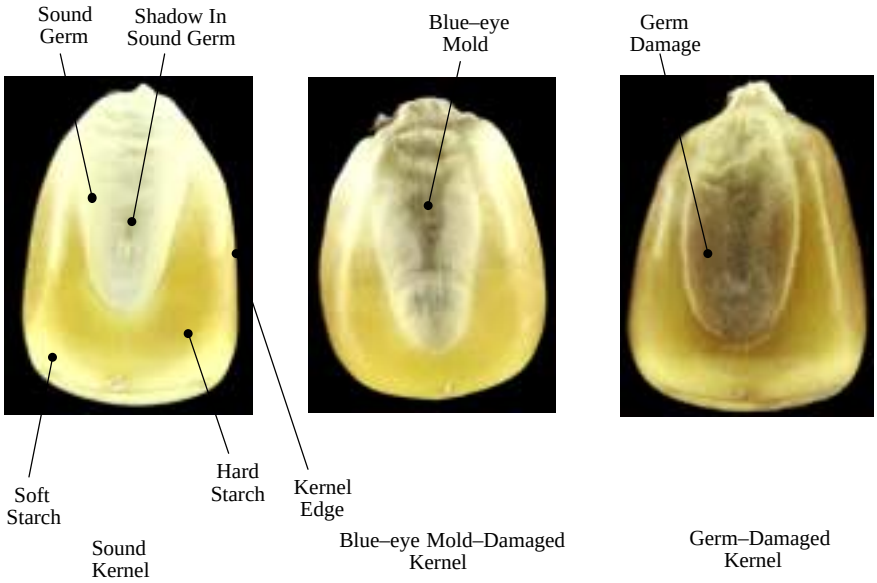

Figure 3. Examples of color pattern categories.

Table 1. Description of color pattern categories.

Attribute Category	Description of Category
Blue-eye mold damage	Areas in blue-eye mold-damaged kernels that represent the color spectrum of blue-eye mold damage. Blue-eye mold damage is a dark bluish purple color and typically appears in the kernel embryo area along the growing point axis and extending to the kernel tip. Blue-eye mold is a fungus that grows under the corn pericarp.
Germ damage	Areas in germ-damaged kernels that represent the typical color spectrum of germ damage. Germ damage is typically expressed by a brownish discoloration throughout the embryo area. Germ damage is caused by respiration (heating) of corn during storage that results in a chemical transformation of the corn embryo.
Sound germ	Areas in sound kernels which represent the typical color spectrum of an undamaged embryo (germ) area
Shadow in sound germ	The three-dimensional nature of a corn kernel places a slight valley down the middle of the embryo region. Shadows from light reflections in this valley caused a slight darkening effect and in preliminary calibrations caused some sound kernels to be misclassified as having blue-eye mold due to color spectrum closeness
Hard starch	Areas in sound kernels which represent the color spectrum of dark (or hard) starch
Soft starch	Areas in sound kernels which represent the color spectrum of light (or soft) starch
Kernel edge	Since corn kernels are three-dimensional in nature, a one to three-pixel transition between the background and kernel will necessarily contain shadows and out-of-focus pixels that are darker than the kernel itself, but lighter than the background.

Table 2. Area of location for selection of attribute categories.

Sound kernels	Hard starch (4 pixel samples)[a] Soft starch (4 pixel samples) Sound germ (4 pixel samples) Shadow in sound germ (4 pixel samples)
Germ-damaged kernels	Germ damage (4 pixel samples)
Blue-eye mold-damaged kernels	Blue-eye mold (4 pixel samples)

[a] Selection of pixel samples was as appropriate. All pixel samples were disconnected. Some images did not have distinct attributes related to the desired class and, therefore, no data were collected for those images. No starch or sound germ samples were taken for germ-damaged or blue-eye mold-damaged kernels. Damaged kernels are likely to have discolorations in other areas of the kernel. The purpose was to get representative data for distinct classifications.

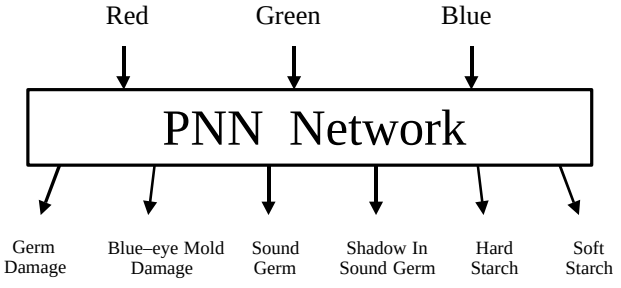

Figure 4. PNN inputs and outputs.

Table 3. Number of pixel samples collected from each attribute catagory.

Attribute Category	No. of Pixel Samples Collected from Image Database
Germ damage	2448
Blue eye mold damage	2424
Sound germ	2465
Shadow in sound germ	2758
Hard starch	2566
Soft starch	1766
Kernel edge	2760

RESULTS AND DISCUSSSION

Histograms of the valid pixel samples collected from each attribute category are given in figure 5. Comparison of the kernel edge histogram with other histograms showed that virtually all pixels with red or green levels less than 32 could be captured in the kernel edge. As a result, a threshold of 32 was applied to the red and green color bands and effectively separated the kernel image from the background.

Table 4 lists the mean and standard deviation of gray levels for each attribute category. As the histograms and statistical measurements show, significant overlap exists between the blue–eye mold and germ damage categories, between sound germ and shadow in sound germ categories, and between hard and soft starch categories. This overlap confused the network model and caused high errors for classification among these categories.

The network weights were first adjusted by a feed forward pass of the training records through the network. An optimal PNN smoothing factor was then selected by applying the trained network to smoothing samples. As previously described, these smoothing samples were not included in the records used for training and validation. Smoothing factor values ranging from 0.001 to 10 were applied, and calculation of correctly classified patterns was performed. As figure 6 shows, percent correct classification predictions for each of the categories varied across the range of the smoothing factor. In general, classification was very poor for smoothing factors of 0.001. As the smoothing factor value increased, classification accuracy reached a maximum and then stabilized to a constant value. Smoothing factors greater than 2 gave very little change in classification. The optimal universal smoothing factor was selected to be 0.05. This value gave the maximum predicted classification accuracy for all categories and near optimal classification accuracy for each individual color pattern group. The smoothing factor value of 0.05 agreed well with the Ward Systems Group's

Table 4. Mean and standard deviation of pixels from each attribute category.

	Mean			Standard Deviation		
Category	Red	Green	Blue	Red	Green	Blue
Germ damage	113	96	45	30	33	25
Blue-eye mold-damaged	128	121	71	33	36	32
Sound germ	233	235	181	10	12	17
Shadow in sound germ	203	201	143	20	24	30
Hard starch	219	206	69	17	21	22
Soft starch	238	237	118	10	12	22
Kernel edge	21	17	4	7	7	6

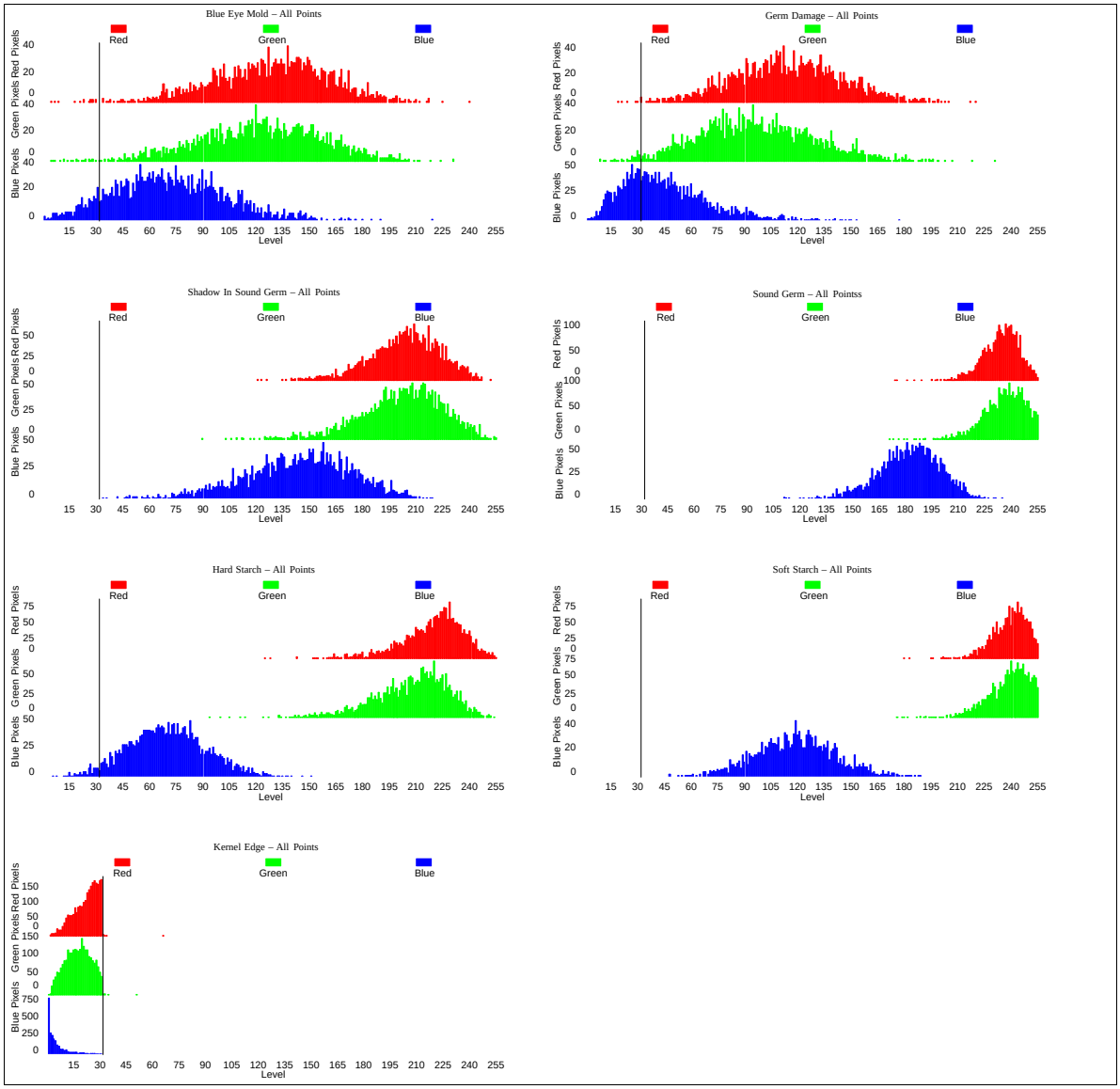

Figure 5. Historgrams of all valid pixel samples collected for eact attribute category (32 selected as a threshold).

(1993) suggestion that good PNN results are usually attained with a smoothing factor value between 0.01 and 1. Classification accuracy on the smoothing samples was 78, 79, 87, 93, 89, and 86% for blue–eye mold, germ damage, shadow in sound germ, sound germ, hard starch, and soft starch, respectively, for an overall classification accuracy of 86%. Overall accuracy of the network on validation records was 75% with 62, 66, 73, 88, 81, and 84% accuracy for blue–eye mold, germ damage, shadow in sound germ, sound germ, hard starch, and soft starch, respectively.

Tables 5a and 5c show contingencies of classification among the smoothing and validation scenarios for application of the smoothing factor σ = 0.05. Most misclassifications were between blue–eye mold and germ damage pixels, between sound germ and shadow in sound germ pixels, and between hard and soft starch pixels. As discussed previously, the spectral histograms showed data overlap in these categories and, therefore, significant network confusion was anticipated.

By adding an additional layer of decision to the network output, which combined similar categories of blue–eye mold and germ damage, sound germ and shadow in sound germ, and hard and soft starch into categories of damage, germ, and starch, the network performance was enhanced. This combination, shown in tables 5b and 5d, shows that the network could predict with high accuracy (97, 98, and 98% for smoothing data; 92, 96, and 96% for validation data) between categories of damage, germ, and starch areas within the corn kernel images (overall accuracy was 98% for smoothing records and 95% for validation data).

Image segmentation using the trained networks was implemented on the image processing system in hardware via values stored in a preprocessed look–up table. Red, green, and blue values from each pixel were mapped to appropriate gray levels for each of the color pattern categories. Pixels having red or green levels less than 32 were mapped to a gray level of 25. For the six–color pattern category scenario, pixels having red, green, blue values corresponding to each

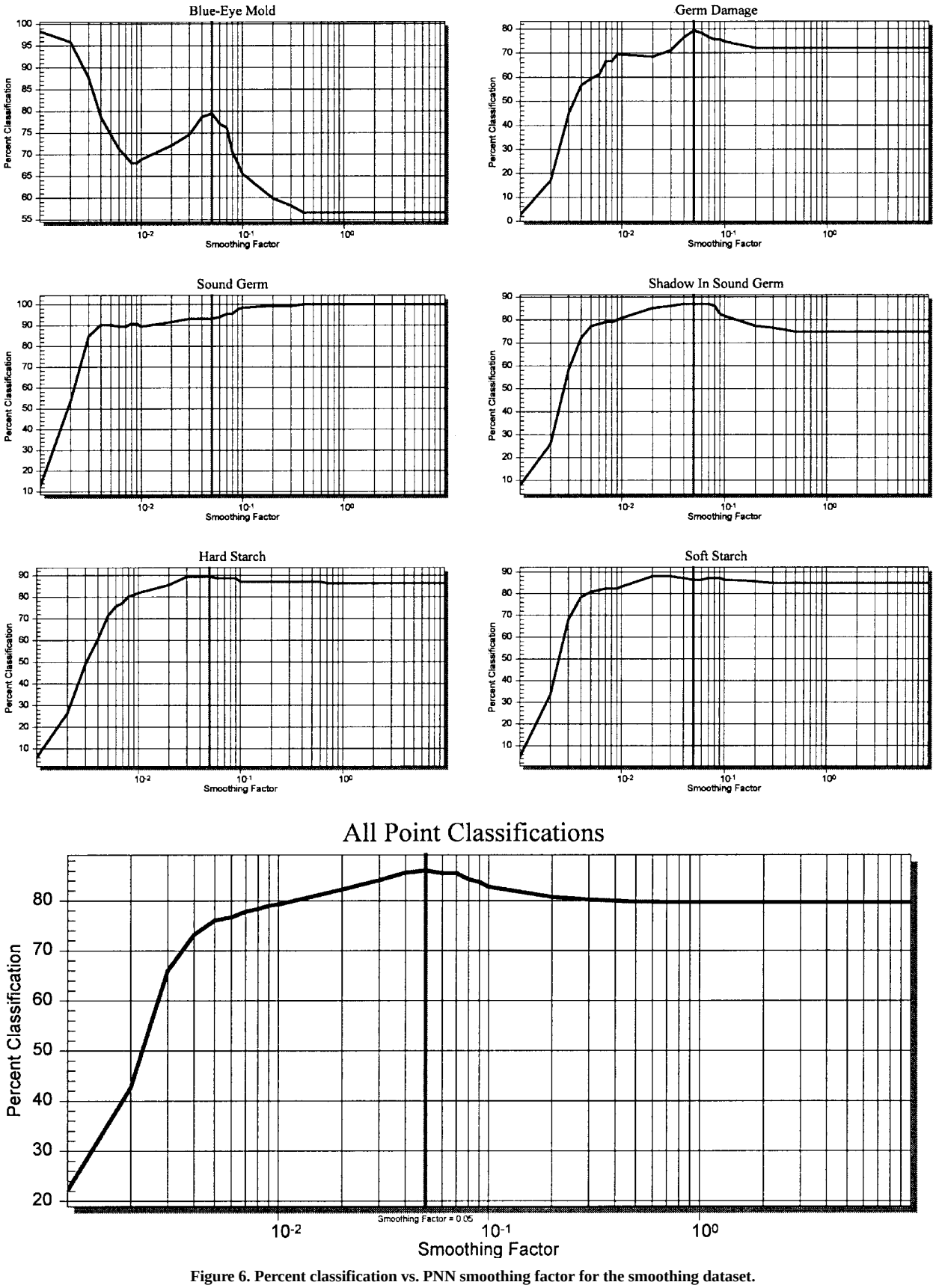

Figure 6. Percent classification vs. PNN smoothing factor for the smoothing dataset.

Table 5a. Agreement matrix for color pattern classifications.[a]

	Actual Blue-Eye Mold	Actual Germ Damage	Actual Shadow in Sound Germ	Actual Sound Germ	Actual Hard Starch	Actual Soft Starch	Total
Classified blue-eye mold	97	20	1	0	0	0	118
Classified germ damage	21	88	0	0	0	0	109
Classified shadow in sound germ	4	3	100	7	0	1	115
Classified sound germ	0	0	12	123	0	4	139
Classified hard starch	0	0	2	0	118	12	132
Classified soft starch	0	0	0	2	14	108	124
Total	122	111	115	132	132	125	737
Correct (%)	78	79	87	93	89	86	86

[a] Smoothing exemplars -- all categories.

Table 5b. Agreement matrix for color pattern classifications.[a]

	Actual Damage	Actual Germ	Actual Starch	Total
Classified as damage	226	1	0	227
Classified as germ	7	242	5	254
Classified as starch	0	4	252	256
Total	233	247	257	737
Correct (%)	97	98	98	98

[a] Smoothing exemplars -- combined categories for damage, germ, starch.

Table 5d. Agreement matrix for color pattern classifications.[a]

	Actual Damage	Actual Germ	Actual Starch	Total
Classified as damage	4047	142	49	4238
Classified as germ	333	4524	98	4955
Classified as starch	4	52	3663	3719
Total	4384	4718	3810	12912
Correct (%)	92	96	96	95

[a] Validation exemplars -- combined categories for damage, germ, starch.

Table 5c. Agreement matrix for color pattern classifications.[a]

	Actual Blue-Eye Mold	Actual Germ Damage	Actual Shadow in Sound Germ	Actual Sound Germ	Actual Hard Starch	Actual Soft Starch	Total
Classified blue-eye mold	1349	695	127	0	33	0	2204
Classified germ damage	555	1448	15	0	16	0	2034
Classified shadow in sound germ	274	54	1836	249	12	8	2433
Classified sound germ	4	1	516	1923	0	78	2522
Classified hard starch	2	2	18	0	1865	158	2045
Classified soft starch	0	0	11	23	374	1266	1674
Total	2184	2200	2523	2195	2300	1510	12,912
Correct (%)	62	66	73	88	81	84	75

[a] Validation exemplars -- all categories.

of the six categories were mapped to arbitrarily assigned gray levels of 100, 125, 150, 175, 200, and 250. For the combined three–color pattern category scenario, pixels were mapped to arbitrarily assigned gray levels of 70, 140, and 210.

Figure 7 shows segmented images of the PNN and optimal smoothing factor applied to each of the corn kernel images displayed in figure 3. The left column displays original color images. The middle column displays segmented images from the six–color pattern category scenario, and the right column displays segmented images from the three–color pattern category scenario. The segmented images show that, in general, color patterns representing corn kernel damage areas can be identified and separated. There are, however, artifacts in the segmentation that were found in Steenhoek et al. (2001) to cause difficulty in using the segmented images for overall kernel classification. For example, in the germ–damaged kernel shown in figure 7, a top–down view of the right side kernel edge is seen by the camera as a dark area misclassified as damage. For the sound kernel example shown in figure 2, light reflections at the kernel crown are seen by the camera as bright areas similar to the white germ area and misclassified as germ area. Similar types of misclassifications were seen in other kernel images. Clearly, the success of this type of segmenting algorithm is dependent on the quality of images to which it is applied.

CONCLUSIONS

An image–processing algorithm for segmentation of damaged and sound areas within corn kernel images was developed. Areas to segment were identified as blue–eye mold, germ damage, sound germ, shadow in sound germ, hard starch, and soft starch. Red, green, and blue pixel values representing each of these areas were sampled from 720 replicate images containing blue–eye mold–damaged, germ–damaged, and sound corn kernels to create a dataset with 14,427 total pixel samples. These 14,427 samples were divided into a 778 sample set for adjustment of network weights, a 737 sample set for adjustment of the probabilistic neural network universal smoothing factor, and a 12,912 sample set for validation of the network. A universal smoothing factor ($\sigma = 0.05$) was selected using the criterion of percent classification of the smoothing dataset. Overall prediction accuracy of the network on validation data was 75% with a large portion of the errors being misclassification between the similar categories of blue–eye mold and germ damage, sound germ and shadow in sound germ, and hard and soft starch. An additional decision layer combining categories of damage, germ, and starch increased classification accuracy to 95% on validation data. Image quality was crucial to the success of this algorithm.

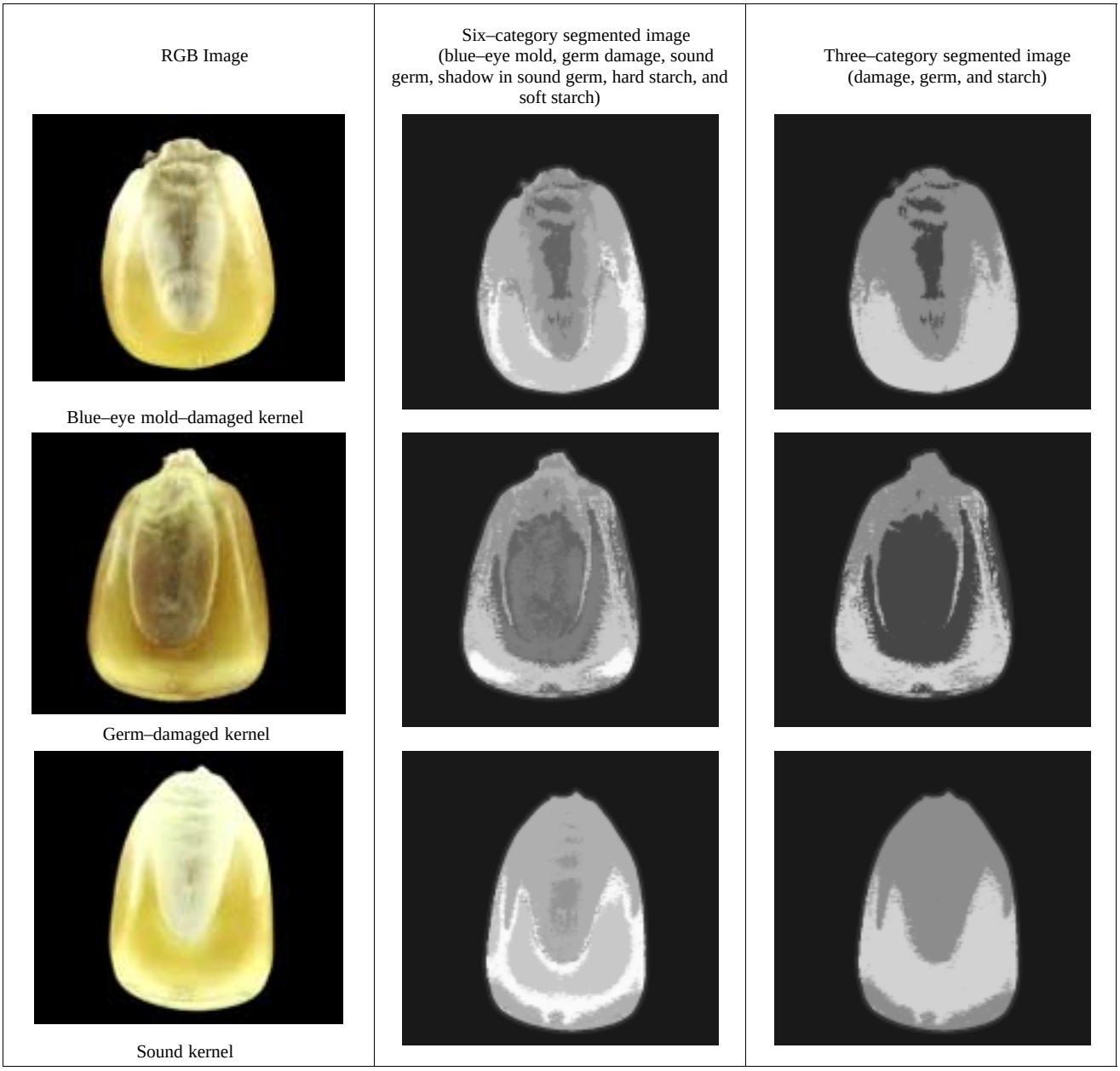

Figure 7. Segmented images.

ACKNOWLEDGEMENTS

Special thanks to the U.S. Federal Grain Inspection Service Board of Appeals and Review for assistance in obtaining corn samples and for sample inspection expertise. Parts of this study were funded by the United States Department of Agriculture, which provided a National Needs graduate fellowship, and by a National Science Foundation grant for machine vision hardware.

REFERENCES

Ahmad, I. S., J. F. Reid, M. R. Paulsen, and J. B. Sinclair. 1993. Soybean seed classification using learning vector quantization. ASAE Paper No. 93–3605. St. Joseph, Mich.: ASAE.

Batchelor, W. D., X. B. Yang, and A. T. Tschanz. 1997. Development of a neural network for soybean rust epidemics. *Transactions of the ASAE* 40(1): 247–252.

Cacoullos, T. 1966. Estimation of a multivariate density. *Annals of Institute of Statistical Mathematics* (Tokyo) 18(2): 179–189.

Chtioui, Y., D. Bertrand, and D. Barba. 1996. Reduction of the size of the learning data in a probabilistic neural network by hierarchical clustering: application to the discrimination of seeds by artificial vision. *Chemometrics and Intelligent Laboratory Systems* 35: 175–186.

Chtioui, Y., S. Panigrahi, and R. Marsh. 1998. Conjugate gradient and approximate Newton methods for an optimal probabilistic neural network for food color classification. *Optical Engineering* 37(11): 1–9.

Dowell, F. E. 1994. Neural network parameter effects on object classification and wavelength selection. *Optical Engineering* 33(8): 2728–2732.

Gao, X., J. Tan, and D. Gerrard. 1995. Image segmentation in 3–dimensional color space. ASAE Paper No. 95–3607. St. Joseph, Mich.: ASAE.

Hush, D. R., and B. G. Horne. 1993. Progress in supervised neural networks, what's new since Lippmann. *IEEE Signal Processing Magazine* 10(1): 8–39.

Jia, J. 1993. Pattern classification of RGB colour images using a BP neural network classifier. *Computer Vision for Industry.* SPIE Vol 1989: 248–295.

Klinker, G. J., S. A. Shafer, and T. Kanade. 1988. Image segmentation and reflection analysis through color. *Applications of Artificial Intelligence VI*. SPIE Vol. 937: 229–244.

Lippmann, R. P. 1987. An introduction to computing with neural nets. *IEEE Acoustics, Speech and Signal Processing Magazine* 4(2): 4–22.

Masters, T. 1993. *Practical Neural Networks in C++*. New York: Academic Press, Inc.

_____. 1995. *Advanced Algorithms for Neural Networks*. New York: John Wiley & Sons, Inc.

McClendon, R. W., and W. D. Batchelor. 1995. An insect pest management neural network. ASAE Paper No. 95–3560. St. Joseph, Mich.: ASAE.

Ng, H. F., W. F. Wilcke, R. V. Morey, and J. P. Lang. 1998. Machine vision color calibration in assessing corn kernel damage. *Transactions of the ASAE* 41(3): 727–732.

Panigrahi, S., D. Wiesenborn, P. Orr, and L. Schaper. 1994. Color classification of french fries using artificial neural network. ASAE Paper No. 94–3561. St. Joseph, Mich.: ASAE.

Panigrahi, S., and R. Marsh. 1996. Neural network techniques for color classification of french fries. ASAE Paper No. 96–3004. St. Joseph, Mich.: ASAE.

Panigrahi, S., C. Doetkott, Y. Chtioui, and R. Marsh. 1998. Computer vision system for color evaluation of edible beans. ASAE Paper No. 98–3053. St. Joseph, Mich.: ASAE.

Precetti, C. J., and G. W. Krutz. 1993a. Real–time color segmentation. ASAE Paper No. 93–3002. St. Joseph, Mich.: ASAE.

_____. 1993b. Building a color classifier. ASAE Paper No. 93–3003. St. Joseph, Mich.: ASAE.

Rumelhart, D. E., and J. L. McClelland. 1986. *Parallel Distributed Processing: Explorations in the Microstructure of Cognition*. *Vol 1. Foundations*. Cambridge, Mass.: MIT Press.

Rumelhart, D. E., B. Widrow, and M. A. Lehr. 1994. The basic ideas in neural networks. *Communications of the ACM* 37(3): 87–91.

Specht, D. F. 1988. Probabilistic neural networks for classification, mapping, or associative memory. IEEE International Conference on Neural Networks, Sheraton Harbor Island, San Diego, Calif., 24–27 July.

_____. 1990. Probabilistic neural networks. *Neural Networks* 3: 109–118.

_____. 1996. Probabilistic neural networks and general regression neural networks. In *Fuzzy Logic and Neural Network Handbook*, ed. C.H. Chen, ch. 3. New York: McGraw–Hill, Inc.

Steenhoek, L. 1999. A probabilistic neural network computer vision system for corn kernel damage evaluation. Ph.D. Diss., Agricultural and Biosystems Engineering Dept., Iowa State University, Ames.

Steenhoek, L., M. Misra, C. Hurburgh, and C. Bern. 2001. Implementing a computer vision system for corn kernel damage evaluation. *Applied Engineering in Agriculture* 17(2): 235–240.

Ward Systems Group. 1993. *NeuroWindows Neural Network Dynamic Link Library.* Frederick, Md.: Ward Systems Group, Inc.

_____. 1997. *NeuroShell Easy Classifier.* Frederick, Md: Ward Systems Group, Inc.

Widrow, B., and M. A. Lehr. 1990. 30 Years of adaptive neural networks: perceptron, madaline, and back–propagation. *Proc. of the IEEE* 78(9): 1415–1441.

Yie, T. J., K. Liao, M. R. Paulsen, and E. B. Maghirang. 1993. Corn kernel stress crack detection by machine vision. ASAE Paper No. 93–3526. St. Joseph, Mich.: ASAE.